Crystal Structure of a Synthetic Triple-Stranded α-Helical Bundle

Brett Lovejoy, Seunghyon Choe, Duilio Cascio, Donald K. McRorie, William F. DeGrado, David Eisenberg*

The x-ray crystal structure of a peptide designed to form a double-stranded parallel coiled coil shows that it is actually a triple-stranded coiled coil formed by three α-helices. Unlike the designed parallel coiled coil, the helices run up-up-down. The structure is stabilized by a distinctive hydrophobic interface consisting of eight layers. As in the design, each α-helix in the coiled coil contributes one leucine side chain to each layer. The structure suggests that hydrophobic interactions are a dominant factor in the stabilization of coiled coils. The stoichiometry and geometry of coiled coils are primarily determined by side chain packing in the solvent-inaccessible interior, but electrostatic interactions also contribute.

A common structural motif of proteins is the α-helical bundle. These bundles appear in different forms, including almost parallel four-α-helical bundles (*1*), crossed bundles (*2*), multiple bundles (*3*), and parallel coiled coils (*4*). The factors that stabilize α-helical bundles and cause a particular protein to adopt one form of bundle over another have not been defined. One experimental approach to defining these factors is the characterization of sequences designed to self-associate into a particular α-helical bundle (*5*). The crystal structure of a 12-residue fragment of a 16-residue peptide designed to form a four-α-helical bundle showed that the peptide is α-helical and self-associates into both a hexameric and tetrameric structure (*6*). Although the structure is more complex than envisioned, it contains the central features of the design: the α-helices are largely stabilized through hydrophobic interactions between leucine side chains.

One class of α-helical bundles stabilized by hydrophobic interactions is the coiled coil, a structure adopted by the proteins keratin, myosin, epidermin, and fibrinogen (*4*). The coiled coil is characterized by a repeating seven-residue pattern. According to the notation of McLachlan and Stewart (*7*), the positions within this heptad repeat are termed a, b, c, d, e, f, and g. From their distinctive x-ray diffraction patterns, Crick inferred that these proteins fold into parallel two- or three-stranded α-helical coiled coils (*8*). He suggested that a "knob" (a hydrophobic side chain) fits into a hole formed by the spaces between side chains of the neighboring helix. The model was confirmed by the crystal structure of a peptide corresponding to the leucine zipper motif of the transcriptional activator GCN4 (*9*). This peptide, GCN4-p1, forms a two-stranded parallel coiled coil in which hydrophobic residues at McLachlan positions a and d fall on the same face of the α-helix. In GCN4-p1 the residues at positions a and d make side-to-side contacts with side chains of the neighboring helix: the side chains of residues at position a pack against side chains of residues at positions a′ and g′ while the side chains of residues at position d pack against side chains of residues d′ and e′ where primed letters refer to positions of the neighboring helix (*9*). This same basic coiled coil structure, both in dimeric and trimeric forms, has been predicted for other transcription factors such as Fos and Jun, and also for heat shock transcription factors (*10*).

Coil-Ser, the subject of this article, was originally designed to provide a model system for evaluating the helix-forming tendencies of the 20 commonly occurring amino acids (*11*). Its sequence originated with the poly-heptapeptide sequence of Hodges and co-workers ($(Leu^aGlu^bAla^cLeu^dGlu^eGly^fLys^g)_n$, which was designed to mimic the two-stranded coiled coil conformation of tropomyosin (*12*) (Fig. 1). In the design of coil-Ser, this heptamer was repeated four times and five amino acid replacements were made in residues other than Leu in order to enhance helical potential (*13, 14*). Potentially destabilizing electrostatic interactions with the helix dipole moment were avoided by blocking the terminal α-NH_3^+ and α-COO^- groups with acetyl and amide groups, respectively (*14*), and Trp^2 and His^{28} were introduced to facilitate nuclear magnetic resonance and ultraviolet spectroscopic studies. As a consequence coil-Ser has, with the single exception of Trp^2, Leu residues occupying positions a and d. This uniform leucine face distinguishes coil-Ser from naturally occurring dimeric coiled coils (*15*), which usually have some smaller residues in these positions.

Structure determination. The initial electron density map of coil-Ser was calculated at 2.5 Å resolution by means of multiple isomorphous replacement (MIR) and the density modification techniques of Zhang and Main (*16*). The quality of the resulting electron density map was sufficient to establish the positions of the polyalanine model of three α-helices and build the side chains for helix I with the use of the program FRODO (*17*). The initial model was subjected to rigid body and positional refinement with subsequent simulated annealing (*18*). Phases from this model were then combined with MIR phases to produce improved $2F_0 - F_c$ maps in which all the side chains of helices II and III were built (Fig. 2A).

X-ray data were collected from an isomorphous crystal of coil-Ser that lacked Gly^{29}; the $F_{coil\text{-}Ser} - F_{coil\text{-}Ser\ desgly}$ difference Fourier map revealed 5σ and 3σ peaks corresponding, respectively, to the $CONH_2$-termini of helices II and III. The $CONH_2$-terminus of helix I is exposed to solvent, with atomic temperature factors for Gly^{29} in excess of 60 $Å^2$, suggesting that the lack of a significant difference peak for this terminus was due to its high mobility. Our model contains all 29 residues of each of the three polypeptide chains and 33 water molecules. It has been refined to an *R* factor of 0.180 for all $F/\sigma(F) \geq 1.0$ data from 7 to 2.1 Å resolution, with root-mean-square (rms) deviations from ideal geometry of 0.017 Å for bond lengths and 2.6° for bond angles (Table 1).

The structure of coil-Ser. Coil-Ser

B. Lovejoy, S. Choe, D. Cascio, and D. Eisenberg are at the Molecular Biology Institute and the Department of Chemistry and Biochemistry, University of California, Los Angeles, Los Angeles, CA 90024–1570. D. K. McRorie is in the Department of Research and Applications, Beckman Instruments, Inc., 1050 Page Mill Road, Palo Alto, CA 94304. W. F. DeGrado is in the Biotechnology Department, DuPont Merck Pharmaceutical Company, P.O. Box 80328, Wilmington, DE 19880–0328.

*To whom correspondence should be addressed.

```
Position  g abcdefg abcdefg abcdefg abcdefg abcdef

Hodges    K LEALEGK LEALEGK LEALEGK LEALEGK LEALEG
GCN4-p1   R MKQLEDK VEELLSK NYHLENE VARLKKL VGER
coil-Ser  E WEALEKK LAALESK LQALEKK LEALEHG
```

Fig. 1. Sequences of coiled coils with heptad positions in the notation of McLachlan and Stewart (*7*): Hodges, the heptamer analog of tropomyosin designed by Hodges repeated four times (*12*); GCN4-p1, the peptide from the protein GCN4 (*9*); coil-Ser, our designed peptide. Coil-Ser has an NH_2-terminal acetyl group and a COOH-terminal carboxamide group. Amino acids are represented by single-letter uppercase abbreviations and McLachlan positions are in lowercase. Residues at the a and d positions are in boldface.

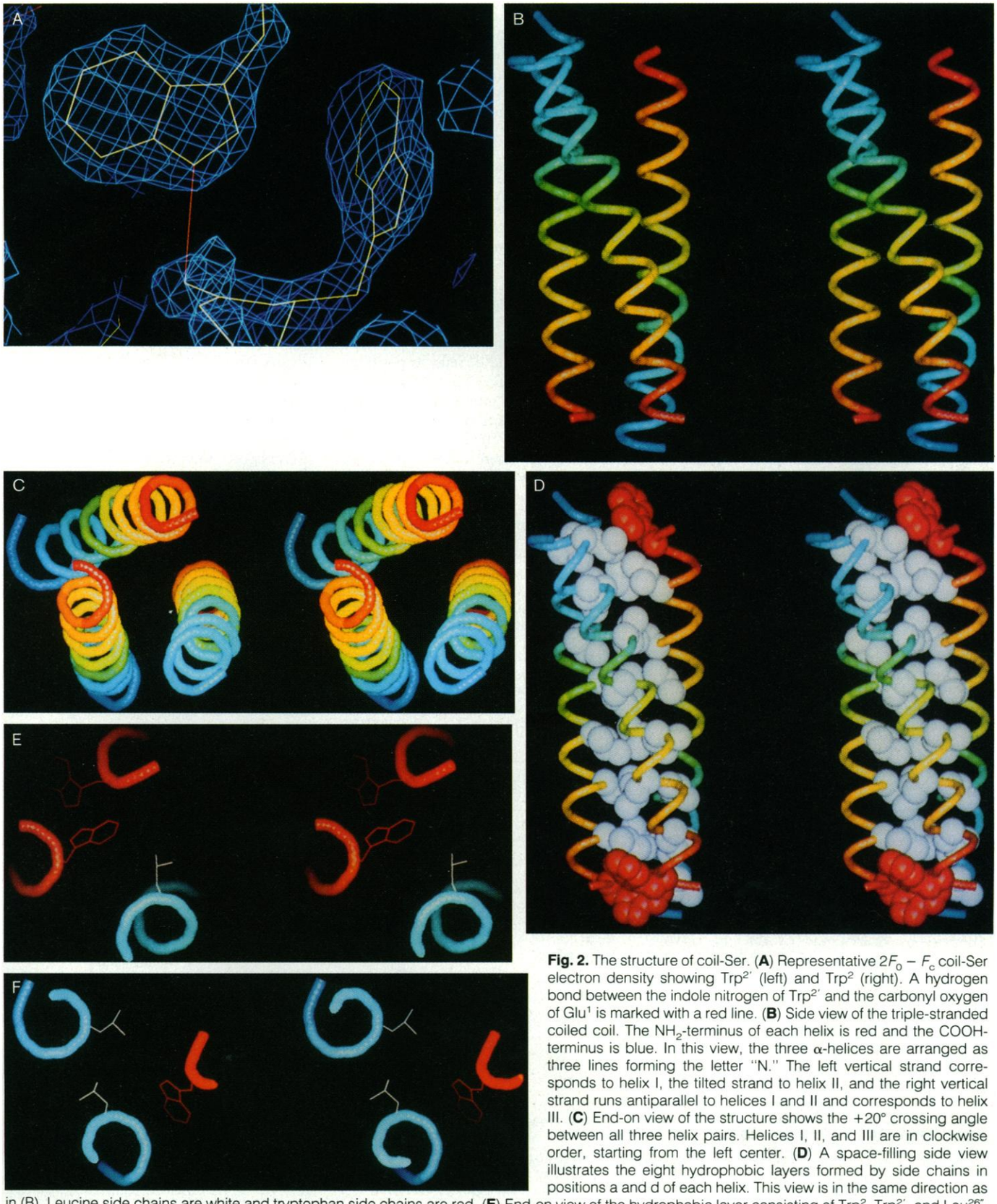

Fig. 2. The structure of coil-Ser. (**A**) Representative $2F_o - F_c$ coil-Ser electron density showing $Trp^{2'}$ (left) and Trp^2 (right). A hydrogen bond between the indole nitrogen of $Trp^{2'}$ and the carbonyl oxygen of Glu^1 is marked with a red line. (**B**) Side view of the triple-stranded coiled coil. The NH_2-terminus of each helix is red and the COOH-terminus is blue. In this view, the three α-helices are arranged as three lines forming the letter "N." The left vertical strand corresponds to helix I, the tilted strand to helix II, and the right vertical strand runs antiparallel to helices I and II and corresponds to helix III. (**C**) End-on view of the structure shows the +20° crossing angle between all three helix pairs. Helices I, II, and III are in clockwise order, starting from the left center. (**D**) A space-filling side view illustrates the eight hydrophobic layers formed by side chains in positions a and d of each helix. This view is in the same direction as in (B). Leucine side chains are white and tryptophan side chains are red. (**E**) End-on view of the hydrophobic layer consisting of Trp^2, $Trp^{2'}$, and $Leu^{26''}$. (**F**) End-on view of the hydrophobic layer consisting of Leu^{26}, $Leu^{26'}$, and $Trp^{2''}$.

forms a triple-stranded α-helical bundle 44 Å in length and 18 Å in diameter (Fig. 2B). All three helices consist of eight helical turns (*19*). Helix I and helix II run in the same direction "up" and helix III runs "down." The three-helix up-up-down topology of coil-Ser has precedents both in globular proteins such as a fragment of protein A where the helices are interconnected by peptide loops (*20*) and in fibrous proteins such as dystrophin and spectrin (*21*). In coil-Ser, the crossing angle between all three helix pairs is about +20°, inducing the three helices to wrap around the superhelical axis to form approximately one-sixth of a turn of a left-handed supercoil (Fig. 2C). The pitch for this supercoil, approximately 270 Å, is long compared to that estimated for fibrous proteins (for example, 140 Å for tropomyosin); this is partly due to the bulky Trp side chains that sterically hinder the termini of the three helices from packing closer together. The distance between the axes of the parallel helices I and II is 11.1 Å, whereas that between the axis of the anti-parallel helix III to the axis of helix I and II is 11.3 and 12.6 Å, respectively. The superhelical trimer axis is straight (Fig. 2C). Sedimentation equilibrium indicates that coil-Ser forms trimers in 0.15 M sodium chloride (pH 7.5) (Fig. 3). The finding that the peptide forms trimers does not affect the earlier calculations of ΔΔG for helix formation (*12*, *22*).

The 16 residues occupying the a and d positions of helices I and II interact with the eight d and a positions of helix III to form a hydrophobic core at the interface of the three α-helices, which consists of eight hydrophobic layers (Fig. 2D). Each layer is formed by interactions of three apolar side chains, the composition of which alternates between d, d′, a″ (Fig. 4A) and a, a′, d″ (Fig. 4B), where a′ and d′ refer to positions on helix II and a″ and d″ refer to positions on helix III. The Cα–Cβ vectors of all leucines occupying a and d positions point toward the superhelical axis (Fig. 2, E and F, and Fig. 4, A and B). In addition, these leucines adopt preferred rotamer angles (χ_1 = gauche plus or trans) with frequencies similar to α-helical leucyl residues in the crystal structures of proteins (*23*).

The occurrence of Trp^2 in a position of the heptad repeat results in three classes of hydrophobic layers in the structure of coil-Ser: Leu-Leu-Leu, Trp-Trp-Leu, and Leu-Leu-Trp. The Trp-Trp-Leu and Leu-Leu-Trp layers occur at each end of the triple-stranded coiled coil, flanking six Leu-Leu-Leu layers. In the Trp^2-$Trp^{2'}$-$Leu^{26''}$ layer, the large size of tryptophan does not leave sufficient room for two tryptophans to occupy the hydrophobic interface (Fig. 2E). As a result $Trp^{2'}$ is forced to face solvent. In this orientation the indole nitrogen of $Trp^{2'}$ forms a hydrogen bond with the carbonyl oxygen of Glu^1 (2.95 Å) (Fig. 2A). In the Leu^{26}-$Leu^{26'}$-$Trp^{2''}$ layer (Fig. 2F), $Trp^{2''}$ is accommodated in the triple-stranded coiled coil hydrophobic interface but is tilted (Fig. 2D). The Cδ carbons of the seven Leu residues occupying the a and d positions of each α-helix are tilted with respect to the plane perpendicular to the superhelical axis. This results in an increase in the hydrophobic interactions between the Leu side chains.

Forces that stabilize coiled coils. Approximately 3900 $Å^2$ of accessible surface area, an area that represents 40 percent of the total accessible surface area, is buried

Table 1. Data collection and phasing statistics. Crystals in space group $P2_12_12_1$ of coil-Ser and of coil-Ser missing Gly^{29} were obtained by precipitation with 2.80 M ammonium sulfate in 0.05 M potassium phosphate buffer that was adjusted to pH 5.0 with sodium hydroxide (*31*). Each x-ray data set was obtained from one crystal with a Rigaku R-AXIS IIC imaging plate. For $Hg(CH_3)_2$ derivatives, crystals were soaked in artificial mother liquor for 6 hours (3.46 M ammonium sulfate in a 0.075 M potassium phosphate buffer that was adjusted to pH 6.6 with sodium hydroxide). Immediately before the data were collected, $Hg(CH_3)_2$ was added by vapor diffusion. For $K_2Pt(SCN)_4$ derivatives, crystals were soaked for 2 days at half the concentration saturated in artificial mother liquor. For $Hg(CH_3)_2$–$K_2Pt(SCN)_4$ double derivatives, crystals were soaked for 5 days with $K_2Pt(SCN)_4$ at half the concentration saturated in artificial mother liquor and then $Hg(CH_3)_2$ was added by vapor diffusion. Anomalous differences were measured for both $Hg(CH_3)_2$-containing derivatives and used in the calculation of MIR phases. Heavy atom parameters were refined and MIR phases were calculated by the program HEAVY (*32*); the mean figure of merit was 0.54 (30 to 2.5 Å).

Data	Native	Native minus Gly^{29}	$Hg(CH_3)_2$	$K_2Pt(SCN)_4$	$Hg(CH_3)_2$ + $K_2Pt(SCN)_4$
Unit cell dimensions (Å)					
a	27.7	28.1	28.0	28.1	28.2
b	38.7	39.3	39.0	39.0	39.0
c	77.8	77.4	77.8	77.5	76.8
Resolution of data (Å)	2.1	2.4	2.5	2.5	2.5
Measured reflections (No.)*	13096	7014	8135	9212	7887
Unique reflections (No.)	4512	2771	2936	2960	2842
Completeness of data (%)†	86	76	92	92	89
R_{merge}‡	0.057	0.056	0.057	0.080	0.057
R_{scale} (8 to 2.5 Å)§		0.17	0.18	0.25	0.30
Number of sites			1	1	2
Rms f_H/ϵ (30 to 2.5 Å)¶			1.17	1.18	1.85
R_{Cullis} (30 to 2.5 Å)‖			0.63	0.61	0.5
Refinement (7 to 2.1 Å)					
R factor**			0.180		
rms bond (Å)			0.017		
rms angle (°)			2.55		
rms dihedral (°)			17.8		

*Only reflections $F/\sigma(F) \geq 1.0$ were processed; *F*, structure factor amplitude. †Percentage of unique data to the resolution limit of the data set. ‡$R_{merge} = \Sigma_i|\langle I_i\rangle - I_i|/\Sigma_i I_i$, and $\langle I_i\rangle$ is the average of I_i over all symmetry equivalents. §$R_{scale} = \Sigma|F_{PH} - F_P|/\Sigma F_P$; F_{PH} and F_P, derivative and native structure factors, respectively. One $Hg(CH_3)_2$ site and one $K_2Pt(SCN)_4$ site (*33*). ¶Rms $f_H/\epsilon = [(\Sigma f_H^2)/\Sigma(F_{PH} - F_P - f_H)^2]^{1/2}$, where f_H is a calculated heavy atom structure factor. ‖$R_{Cullis} = \Sigma|F_{PH} - F_P - f_H|/\Sigma|F_{PH} - F_P|$ for centric reflections. **Refinement with X-PLOR (*18*) resulted in an *R* factor of 0.211 against all $F/\sigma(F) \geq 1.0$ data from 7 to 2.1 Å resolution. The rms deviations from ideal bonds and angles were 0.016 Å and 2.66°, respectively. The *R* factor against the same data, 4198 reflections, with a single isotropic thermal parameter and no solvent molecules, had an *R* factor of 0.283. Refinement was continued with TNT (*34*) to yield a model having an *R* factor of 0.180 against all $F/\sigma(F) \geq 1.0$ data from 7 to 2.1 Å resolution.

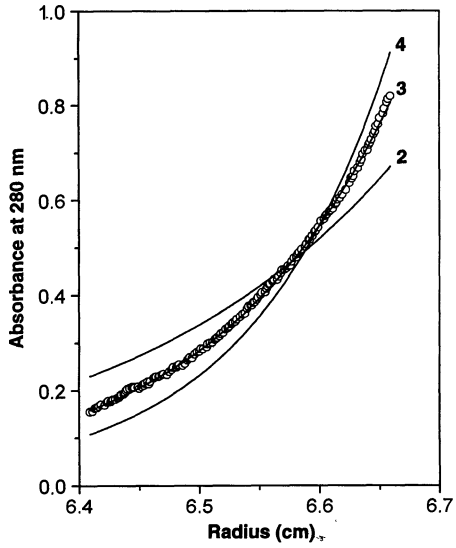

Fig. 3. Analytical ultracentrifugation of coil-Ser. The analysis was performed in a Beckman XL-A analytical ultracentrifuge at 20°C with a loading concentration of 0.2 mg/ml in 10 mM 3-[*N*-morpholino]propane-sulfonic acid (MOPS), 150 mM sodium chloride, pH 7.5. Shown by circles is the concentration distribution as a function of radial position of coil-Ser at equilibrium after 24 hours at 30,000 rpm. The data fit best for a single species with a molecular size of 10,258 daltons (curve 3), a value in close agreement with the calculated molecular size for the trimer of 10,040 daltons. For comparison, curves for a dimer (curve 2) and tetramer (curve 4) are shown. Analyses of residual differences from curve 3 do not reveal systematic error.

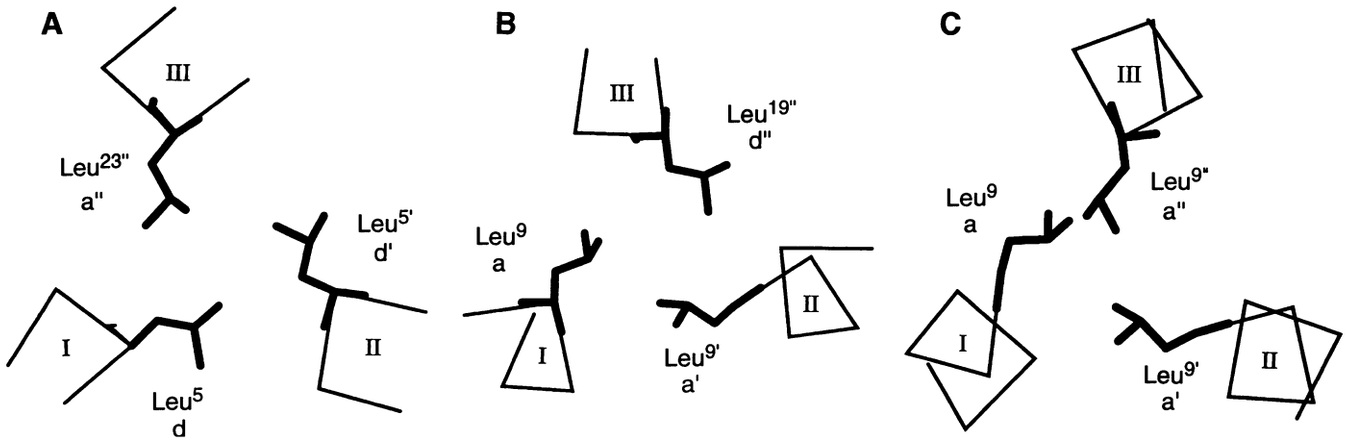

Fig. 4. An end-on view of the Leu-Leu-Leu hydrophobic layer illustrates how the tendency of Leu to adopt negative χ_1 angles causes the Cβ-Cγ bond of each Leu side chain occupying d positions to bend away from the superhelical axis and the Cβ-Cγ bond of each Leu side chain occupying a positions to bend toward the superhelical axis. The two types of hydro- phobic layers observed in the coil-Ser structure are represented by (**A**) Leu^5-$Leu^{5'}$-$Leu^{23''}$ (d-d′-a″) and (**B**) Leu^9-$Leu^{9'}$-$Leu^{19''}$ (a-a′-d″). (**C**) In a hypothetical representation of coil-Ser as an all parallel triple-stranded coiled coil, the residues Leu^9, $Leu^{9'}$, and $Leu^{9''}$ form a hydrophobic layer of the type a-a′-a″. This panel illustrates how the adoption of favorable χ_1 angles by Leu in this type of layer causes their side chains to collide. Such collisions can be avoided by the adoption of less favorable χ_1 angles by Leu.

when the trimer is formed from helical monomers (*24*). This change results in a gain in hydrophobic stabilization energy. On the basis of hydrophobic potential energy calculations (*25*), both GCN4-p1 and coil-Ser form the most stable structures possible. GCN4-p1 tends toward dimer formation rather than trimer formation, and coil-Ser is more stable as an up-up-down triple-stranded coiled coil than as an all parallel triple-stranded or double-stranded coiled coil (Table 2) although the energy differences are small. Thus the hydrophobic stabilization energy provides the main driving force for the formation of coiled coils from helical monomers and may even influence the stoichiometry and strand polarity of coiled coils.

Like GCN4-p1, coil-Ser is stabilized by three interhelical salt bridges between charged residues in the e and g positions of the heptad repeat (Fig. 5) (*26*). Such salt bridges are believed to stabilize naturally occurring double-stranded coiled coils (*4*) and are found in GCN4-p1. Coil-Ser is also stabilized by an additional interhelical salt bridge between charged residues in the g and b positions as well as four intrahelical salt bridges (*26*). An unexpected feature of the coil-Ser structure is the grouping of like charges between the e and g positions of antiparallel helices (Fig. 5B). Examination of the structure reveals that these charged side chains have sufficient conformational flexibility to move away from each other. The presence of interhelical salt bridges between helix I and II only, and also the presence of unexpected repulsive interactions, suggest that interhelical salt bridges are not a dominant driving force in the formation of coiled coils but rather an indirect consequence of coiled coil formation. Our findings are consistent with the studies of α-tropomyosin by Skolnick and Holtzer, in which they propose that the

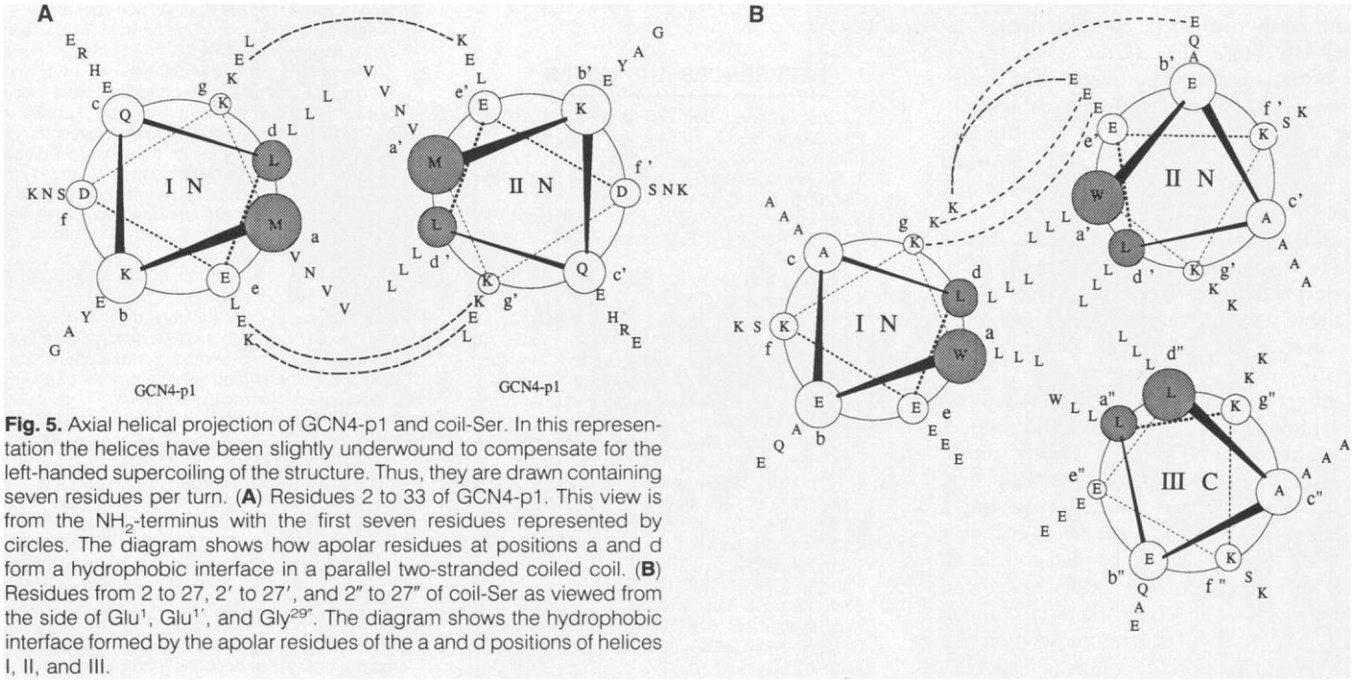

Fig. 5. Axial helical projection of GCN4-p1 and coil-Ser. In this representation the helices have been slightly underwound to compensate for the left-handed supercoiling of the structure. Thus, they are drawn containing seven residues per turn. (**A**) Residues 2 to 33 of GCN4-p1. This view is from the NH_2-terminus with the first seven residues represented by circles. The diagram shows how apolar residues at positions a and d form a hydrophobic interface in a parallel two-stranded coiled coil. (**B**) Residues from 2 to 27, 2′ to 27′, and 2″ to 27″ of coil-Ser as viewed from the side of Glu^1, $Glu^{1'}$, and $Gly^{29''}$. The diagram shows the hydrophobic interface formed by the apolar residues of the a and d positions of helices I, II, and III.

Table 2. Atomic solvation (hydrophobic) energy calculations for coil-Ser and GCN4 structures, based on the method of Eisenberg and McLachlan and the atomic solvation parameters of Eisenberg *et al.* (*25*). The net hydrophobic stabilization energy for each structure was derived by subtracting the energy of component α helices from the energy of the complete structure.

Model	Net hydrophobic stabilization energy (kcal/mol)	Net hydrophobic stabilization energy per helix (kcal/mol)
Coil-Ser structure	−33.7	−11.2
All parallel coil-Ser model*	−32.0	−10.7
GCN4 structure (*9*)	−19.0	−9.5
GCN4 model with coil-Ser sequence*	−19.1	−9.6
Coil-Ser model with GCN4 sequence*	−19.4	−6.5

*The GCN4 model with the coil-Ser sequence and the coil-Ser model with residues 1 through 29 of the GCN4 sequence were created by mutating the respective GCN4 and coil-Ser crystal structures with the use of the program FRODO (*17*). The all parallel coil-Ser structure was created by docking helix III to helices I and II in an all parallel orientation. All model coordinates were subjected to positional refinement with X-PLOR (*18*) before hydrophobic energy calculations were made.

influence of interhelical salt bridges to coiled coil stabilization is small compared to that of hydrophobic interactions (*27*).

The polarity of coil-Ser. The small difference in hydrophobic stabilization energy that coil-Ser gains by forming an up-up-down trimer rather than an all parallel trimer (Table 2) suggests that additional factors may influence the polarity of coil-Ser and coiled coils in general. One such factor might be the interactions of the macrodipole moment (*28*) of the helices. The up-up-down polarity of coil-Ser could provide electrostatic stabilization energy in the form of favorable interactions between dipole moments of antiparallel α-helical pairs (helix I and II, helix I and III), as suggested by Hol *et al.* (*29*). In addition, the up-up-down polarity of coil-Ser allows Leu residues in the a position of helix III to adopt favorable rotamer angles. To avoid steric clash, an all parallel trimer would require Leu residues in the a position to adopt energetically less favorable χ_1 angles (Fig. 4C).

While a modest improvement in hydrophobic stabilization energy, favorable packing of Leu side chains in the a position of helix III and favorable interactions between helix dipole moments may influence the polarity adopted by coil-Ser, one must also consider that an all parallel trimer would result in a Trp-Trp-Trp layer, resulting in steric clash. At present we are unable to evaluate the relative influence of hydrophobic, steric, and electrostatic factors on the polarity of the coil-Ser structure.

Effect of a and d positions on coiled coil stoichiometry. The nature of the residues at positions a and d of the heptad repeat influences the stoichiometry of α-helical bundles, with Leu in position a favoring a triple-stranded up-up-down coiled coil over a double-stranded parallel coiled coil. In an extensive survey of two-stranded coiled coil proteins Lupas and co-workers (*30*) found that Leu is, by far, the most preferred residue at position d, whereas Leu, Ile, Met, and Val are all relatively well tolerated at position a. The structure of coil-Ser demonstrates that what distinguishes Leu from Ile, Met, and Val in the a position is a combination of its steric properties (with two Cδ carbons) and its strict preference for negative χ_1 angles (Fig. 4). The absence of Leu in the a positions of GCN4-p1 is consistent with our modeling studies that show that adoption of this favored χ angle by Leu in the a position of double-stranded parallel coiled coils results in a steric clash similar to that shown in Fig. 4C. Of course, Leu can occur in the a position of parallel coiled coils if it adopts a less favored rotamer. Analysis of peptide analogs of coil-Ser, in which the Trp and Leu occupying the a positions are replaced by Val or Ile, will shed further light on the effect of hydrophobic residues on the stoichiometry and polarity of coiled coils. These replacements may stabilize a double-stranded parallel coiled coil.

REFERENCES AND NOTES

1. C. Chothia, *Annu. Rev. Biochem.* **53**, 537 (1984); P. C. Weber and F. R. Salemme, *Nature* **287**, 81 (1980).
2. T. C. Terwilliger and D. Eisenberg, *J. Biol. Chem.* **257**, 6016 (1982).
3. S. E. Ealick *et al.*, *Science* **252**, 698 (1991); R. Huber, J. Römich, E.-P. Paques, *EMBO J.* **9**, 3867 (1990).
4. C. Cohen and D. A. D. Parry, *Proteins Struct. Funct. Genet.* **7**, 1 (1990).
5. D. Eisenberg, W. Wilcox, S. M. Eshita, P. M. Pryciak, S. P. Ho, W. F. DeGrado, *ibid.* **1**, 16 (1986); W. F. DeGrado, L. Regan, S. P. Ho, *Cold Spring Harbor Symp. Quant. Biol.* **52**, 521 (1987).
6. C. P. Hill, D. H. Anderson, L. Wesson, W. F. DeGrado, D. Eisenberg, *Science* **249**, 543 (1990).
7. A. D. McLachlan and M. Stewart, *J. Mol. Biol.* **98**, 293 (1975).
8. F. H. C. Crick, *Acta Crystallogr.* **6**, 689 (1953).
9. E. K. O'Shea, J. D. Klemm, P. S. Kim, T. Alber, *Science* **254**, 539 (1991); the crystal structure of GCN4 complexed with DNA has been reported by T. E. Ellenberger, C. J. Brandl, K. Struhl, and S. C. Harrison [*Cell* **71**, 1223 (1993)].
10. E. K. O'Shea, R. Rutkowski, W. F. Stafford III, P. S. Kim, *Science* **245**, 646 (1989); P. K. Sorger and H. C. M. Nelson, *Cell* **59**, 807 (1989); O. Perisic, H. Xiao, J. T. Lis, *ibid.*, p. 797.
11. K. T. O'Neil and W. F. DeGrado, *Science* **250**, 646 (1990). The physical properties of amino acids were studied by substituting them for residue 14 in the designed sequence. This resulted in a series of peptides named coil-x, where x is the amino acid at position 14.
12. R. S. Hodges, A. K. Saund, P. C. S. Chong, S. A. St.-Pierre, R. E. Reid, *J. Biol. Chem.* **256**, 1214 (1981). Sedimentation equilibrium of the parent polyheptapeptides [S. Y. M. Lau, A. K. Taneja, R. S. Hodges, *J. Biol. Chem.* **259**, 13253 (1984)] had suggested that coil-Ser should form dimers, and sedimentation equilibrium by the airfuge method [R. J. Pollet, B. A. Hasse, M. L. Standaert, *ibid.* **254**, 30 (1979)] also confirmed this result for a peptide closely related to coil-Ser (*11*). However, we were not able to use airfuge centrifugation reliably for a peptide of this size.
13. P. Y. Chou and G. D. Fasman, *Adv. Enzymol.* **47**, 45 (1978).
14. S. Marquèsee and R. L. Baldwin, *Proc. Natl. Acad. Sci. U.S.A.* **84**, 8898 (1987).
15. J. F. Conway and D. A. D. Parry, *Int. J. Biol. Macromol.* **12**, 328 (1990); D. A. D. Parry, *Biosci. Rep.* **2**, 1017 (1982).
16. K. Y. J. Zhang and P. Main, *Acta Crystallogr. Sect. A* **46**, 41 (1990); *ibid.*, p. 377.
17. T. A. Jones, *Methods Enzymol.* **115**, 157 (1985).
18. A. T. Brünger, A. Krukowski, J. W. Erickson, *Acta Crystallogr. Sect. A* **46**, 585 (1990).
19. Glu^1, His^{28}, and Gly^{29} are extended rather than in α-helical conformation. The main chain dihedral angles, phi and psi, for residues 2 to 27 range from −87° to −47° and from −69° to −7° and are clustered around −64° and −41°, respectively. After superposition, the rms deviations between Cα carbons constituting the α-helical portion of coil-Ser, residues 2 to 27, of helix I and II, helix I and III, and helix II and III are 0.86 Å, 0.83 Å, and 0.35 Å, respectively. The close agreement of helix II and III occurs because both α-helices bend approximately 10 degrees in the vicinity of Ser^{14} and Lys^{15}. Thus the Cα carbons in the residue range 2 to 14 of helix I, which is straight, can be superimposed on helix II and III with an rms deviation of 0.30 and 0.32 Å, respectively, while residues 15 to 27 of helix I can be superimposed on helix II and III with an rms deviation of 0.39 and 0.50 Å, respectively.
20. J. Deisenhofer, T. A. Jones, R. Huber, J. Sjödahl, J. Sjöquist, *Hoppe-Seylers Z. Physiol. Chem.* **359**, 975 (1978).
21. J. F. Conway and D. A. D. Parry, *Int. J. Biol. Macromol.* **13**, 15 (1991); D. W. Speicher and V. T. Marchesi, *Nature* **311**, 177 (1984); M. D. Davison and D. R. Critchley, *Cell* **52**, 159 (1988).
22. Sedimentation analysis of coil-Ser, coil-D-Ala, and coil-Trp in 5.0 M urea [the conditions were those used in (*11*)] indicates that this class of peptides can exist in a sequential monomer-dimer-trimer equilibrium. Reestimation of the monomer-dimer equilibrium constants by fitting the data in (*11*) to a monomer-dimer-trimer scheme has provided estimates of ΔΔG that are identical to earlier estimates (W. DeGrado, J. Lear, R. Fairman, D. McRorie, in preparation).
23. M. J. McGregor, S. A. Islam, M. J. E. Sternberg, *J. Mol. Biol.* **198**, 295 (1987).
24. The docking of helix I to II, I to III, and II to III contributes equally to the total surface area buried when coil-Ser is formed. Surface area calculations were performed with the program X-PLOR (*18*) with a probe radius of 1.6 Å.
25. D. Eisenberg and A. D. McLachlan, *Nature* **319**, 199 (1986); D. Eisenberg, M. Wesson, M. Yamashita, *Chem. Scr.* **29A**, 217 (1989).
26. Distances between charged groups suggest that interhelical salt bridges form between Lys^8 and Glu$^{13'}$ (2.6 Å), Lys^{15} and Glu$^{20'}$ (4.0 Å), Lys^{22} and Glu$^{24'}$ (2.8 Å), and Lys^{22} and Glu$^{27'}$ (3.6 Å). Distances between charged groups suggest that intrahelical ion pairs form between Glu^3 and Lys^7 (3.0 Å), Glu$^{24'}$ and His$^{28'}$ (3.7 Å), Glu$^{27'}$ and His$^{28'}$ (2.9 Å), and Glu$^{24''}$ and His$^{28''}$ (2.4 Å). The average distance between the six interhelical pairs containing like charges in positions e and g is 7.7 Å.

27. J. Skolnick and A. Holtzer, *Macromolecules* **18**, 1549 (1985).
28. W. G. J. Hol, P. T. van Duijnen, H. J. C. Berendsen, *Nature* **273**, 443 (1978).
29. W. G. J. Hol, *Prog. Biophys. Mol. Biol.* **45**, 149 (1985).
30. A. Lupas, M. Van Dyke, J. Stock, *Science* **252**, 1162 (1991).
31. B. Lovejoy *et al.*, *Protein Sci.* **1**, 956 (1992).
32. T. C. Terwilliger and D. Eisenberg, *Acta Crystallogr. Sect. A* **39**, 813 (1983).
33. The Pt site is within covalent bonding distance to $His^{28'}$; Hg occupies a crevice formed by Glu^{20}, Glu^{24}, Glu^{27}, and $Glu^{6''}$ as well as symmetry-related $Glu^{1''}$.
34. D. E. Tronrud, L. F. TenEyck, B. W. Matthews, *Acta Crystallogr. Sect. A* **43**, 489 (1987).
35. We thank T. Alber for providing coordinates of the GCN4-p1 dimer, A. Rockwell for the synthesis and purification of coil-Ser, and C. Cohen and T. Alber for discussions. The coordinates have been deposited with the Brookhaven Protein Database (access number 1COS). Supported by grants from the NIH (31299), NSF (DMB 8913316), and the Lita Annenberg Hazen Charitable Trust.

5 November 1992; accepted 19 January 1993